

Effect of sodium chloride on yield, purity, morphology and polymorphs of calcium or magnesium carbonate sequentially precipitated from brine solution

Naswibu A. Kasimu^{a,b,*}, Jun Gu^{a,*}

^a Department of Petroleum Engineering, Faculty of Earth Resources, China University of Geoscience, Wuhan, China

^b Chemistry Department, P.O. Box 35061, University of Dar es Salaam, Tanzania

HIGHLIGHTS

- Study shows the effect of 0.0 M to 2.0 M NaCl on precipitation calcium or magnesium carbonates from oilfield brine.
- The concentration of 1 M NaCl offered maximum yield and purity of the precipitates.
- 0–0.5 M NaCl favored more precipitation of aragonite and calcite whereas 1–2 M NaCl favored aragonite, vaterite, and calcite.
- 0.0 M to 2.0 M NaCl did not change the polymorph of magnesium carbonate only it affected its morphology.
- The findings show that CaCO_3 or $\text{MgCO}_3 \cdot 3\text{H}_2\text{O}$ can be produced from oilfield brine for various industrial applications.

ARTICLE INFO

Keywords:

Brine solution
Sequential precipitation
Purity
Morphology
Polymorph

ABSTRACT

Oilfield brine disposal in marine environments is undesirable due to concentrated salts of calcium, magnesium, sodium, and others which endanger aquatic organisms. Thus, it is paramount to precipitate the dissolved ions into stable carbonates for industrial applications. However, the effect of NaCl in the brine solution on the quantity and quality of precipitated carbonates is not yet reported. In this study, microwave plasma atomic emission spectrometer (MIP AES), x-ray diffraction (XRD), and scanning electron microscopy (SEM) were employed to investigate the effect of 0–2 M NaCl on the yield, purity, polymorph, and morphology of calcium and magnesium carbonates. The yields of 96.2% to 98.9% and 53.7% to 69.6% and the purity of 90.9% to 92.7% and 96% to 99.5% CaCO_3 and $\text{MgCO}_3 \cdot 3\text{H}_2\text{O}$ were obtained, respectively. Moreover, the maximum yield and purity of carbonates were obtained from a brine solution of 1 M NaCl. The concentration of 0–0.5 M NaCl favored more the formation of aragonite whiskers and rhombohedral calcite whereas the concentration of 1–2 M NaCl favored more the formation of aragonite whiskers, lamella vaterite, and rhombohedral calcite. Nevertheless, only nesquehonite ($\text{MgCO}_3 \cdot 3\text{H}_2\text{O}$) precipitated regardless of brine concentration. The crystal surface and length of the precipitated nesquehonite from 1 to 2 M NaCl brine were affected.

1. Introduction

Water flooding and other oil enhancement methods are frequently used to enhance the recovery of crude oil from aged oil wells. American Petroleum Institute (API) estimated that nine barrels of water can be produced for each barrel of oil during crude oil production [1]. Depending on the nature of geological formations, the oilfield brine and produced water come out of the reservoir with dissolved ions such as Na^+ , Ca^{2+} , and Mg^{2+} [2–6]. It is common practice to dispose of oilfield

brine (produced water) into water bodies. However, this approach is not safe for plants and animals' lives [1,5]. When brine is disposed of in water bodies, it can change the salinity and pH of water, causing the death of aquatic organisms [1,7]. For that reason, many environmental regulatory bodies for example, Environmental Protection Agency (EPA) have set regulations that require the oil brine solutions or produced water to be treated before disposal into water bodies [1,8].

Precipitation as an alternative method for brine treatment has attracted many researchers nowadays due to its low cost while solving

* Corresponding author at: Department of Petroleum Engineering, Faculty of Earth Resources, China University of Geosciences, Wuhan, China.

E-mail addresses: naswibu2018@gmail.com (N.A. Kasimu), gujun@cug.edu.cn (J. Gu).

<https://doi.org/10.1016/j.desal.2024.117443>

Received 29 July 2023; Received in revised form 14 February 2024; Accepted 15 February 2024

Available online 19 February 2024

0011-9164/© 2024 Elsevier B.V. All rights reserved.

Table 1
Concentrations of major cations in produced water from oilfields per world.

Range of concentrations in different oil fields			References
Ca ²⁺ (Mg/L)	Mg ²⁺ (mg/L)	Na ⁺ (mg/L)	
13–29,222	8–600	132–97,000	[21]
4–78,000	2–7000	850–20,000	[22]
13–74,000	8–6000	132–150,000	[23]
416–26,000	1294–8400	10,760–120,000	[24]
13–30,800	<8–10,000	50–29,700	[25]
0–74,000	0–6000	0–150,000	[26]

Table 2
Composition of synthetic brine solution used in study.

Experiment	CaCl ₂		MgCl ₂ ·6H ₂ O		NaCl
	CaCl ₂ [M]	Ca ²⁺ (mg/L)	MgCl ₂ ·6H ₂ O [M]	Mg ²⁺ (mg/L)	NaCl [M]
1	0.5	20,000	0.4	10,000	0.0
2	0.5	20,000	0.4	10,000	0.5
3	0.5	20,000	0.4	10,000	1.0
4	0.5	20,000	0.4	10,000	1.5
5	0.5	20,000	0.4	10,000	2.0

Table 3
Precipitating reagents tested in preliminary precipitation of carbonates.

Experiment	Precipitating reagents	Weight (g)	Concentration [M]
1	NaHCO ₃	10.5	0.5
2	NaHCO ₃	16.8	0.8
3	NaHCO ₃ /Na ₂ CO ₃	12.6/5.3	0.6/0.2
4	NaHCO ₃	21.0	1.0
5	NaHCO ₃ /Na ₂ CO ₃	21.0/5.3	1.0/0.2
6	Na ₂ CO ₃	26.5	1.0

environmental challenges [9]. Through the precipitation method, high-purity mineral carbonates can be produced for industrial applications. Calcium carbonate, for example, is used in papers, cosmetics, toiletries, food, pharmaceuticals, plastics, paints, inks, sealants, and adhesives [10]. On the other hand, hydrated magnesium carbonate compounds like nesquehonite (MgCO₃·3H₂O) can be used in the production of construction materials such as thermally insulating boards, blocks, and panels [11]. Thus, it is important to recover these mineral carbonates from oilfield brine solution or produced water.

Table 4
Preliminary findings of CaCO₃ based precipitates at 25 °C and 50 °C.

Experiment	Precipitating reagents	Concentration [M]	Precipitation temperature (25 °C)		Precipitation temperature (50 °C)	
			%Yield	%Purity	%Yield	%Purity
1	NaHCO ₃	0.5	55.4	82.8	82.4	86.6
2	NaHCO ₃	0.8	57.1	84.0	78.0	87.7
3	NaHCO ₃ /Na ₂ CO ₃	0.6/0.2	72.9	84.7	85.6	89.4
4	NaHCO ₃	1.0	85.6	85.9	85.6	88.7
5	NaHCO ₃ /Na ₂ CO ₃	1.0/0.2	95.6	88.7	96.2	91.0
6	Na ₂ CO ₃	1.0	93.5	83.3	94.8	90.0

Table 5
Preliminary findings of MgCO₃·3H₂O based precipitates at 25 °C and 50 °C.

Experiment	Precipitating reagents	Concentration [M]	Precipitation temperature (25 °C)		Precipitation temperature (50 °C)	
			%Yield	%Purity	%Yield	%Purity
1	NaHCO ₃	0.5	34.4	59.8	50.1	82.9
2	NaHCO ₃	0.8	84.4	61.4	51.5	77.4
3	NaHCO ₃ /Na ₂ CO ₃	0.6/0.2	52.9	65.6	52.0	85.7
4	NaHCO ₃	1.0	77.0	78.3	52.9	93.1
5	NaHCO ₃ /Na ₂ CO ₃	1.0/0.2	34.4	88.9	54.1	95.5
6	Na ₂ CO ₃	1.0	32.2	86.8	53.5	95.8

Different types of polymorphs of carbonates can be precipitated depending on the conditions used. For examples, magnesium carbonates can exist as magnesite (MgCO₃), nesquehonite (MgCO₃·3H₂O), dypingite (Mg₅(CO₃)₄(OH)₂·5H₂O), hydromagnesite (Mg₅(CO₃)₄(OH)₂·4H₂O), Lansfordite (MgCO₃·5H₂O) and Artinite (MgCO₃·Mg(OH)₂·3H₂O) [12,13]. On the other side, calcium carbonate can exist as calcite, vaterite, aragonite, and hydrated compounds like ikaite (CaCO₃·6H₂O) and monohydrated calcium carbonate (CaCO₃·H₂O) [14–16]. Different past research focused on the precipitation of calcium or magnesium-based carbonates from various sources. The combination of Na₂CO₃ solutions in equilibrium with a CO₂ atmosphere and MgCl₂ solutions resulted in precipitation of MgCO₃·3H₂O at 25 °C and PCO₂ = 1 bar, hydromagnesite ((Mg₅CO₃)₄ Mg(OH)₂·4H₂O) at 120 °C and PCO₂ = 100 bar, and magnesite MgCO₃ at 120 °C and PCO₂ = 100 bar [12]. MgCO₃·3H₂O was prepared by using brine rich in Mg from the desalination plant, CO₂, and NaOH at 20 °C to 25 °C and atmospheric pressure [11]. Nevertheless, >95 % of calcium was converted into CaCO₃ by reacting phosphogypsum with NH₃ and CO₂ at ambient conditions [17]. Costa and Teir (2016) [18] prepared CaCO₃ by reacting steelmaking slag as a raw material with NH₄Cl and CO₂. Other research shows that >99.4 % pure CaCO₃ can be produced by reacting CO₂, cement kiln dust, and seawater [19]. CaCO₃ and MgCO₃·3H₂O were prepared from seawater by reacting CO₂, MgO, and NaOH at 80 °C [20]. Based on our knowledge and level of literature survey, the effect of NaCl on the yield, purity, polymorphs, and morphology of the precipitated carbonates is not yet known. Therefore, we conducted an experimental study to investigate the effect of varying the concentration of NaCl on the yield, purity, polymorphs, and morphology of calcium and magnesium carbonates obtained by sequential precipitation.

Table 6
Initial and final pH during sequential precipitation of carbonates.

Experiment	NaCl [M]	First precipitation step		Second precipitation step	
		Initial pH	Final pH	Initial pH	Final pH
1	0.0	8.93	4.01	3.99	9.72
2	0.5	8.72	3.93	3.96	9.61
3	1.0	8.51	3.87	3.92	9.53
4	1.5	8.32	3.68	3.83	9.45
5	2.0	8.21	3.56	3.71	9.32

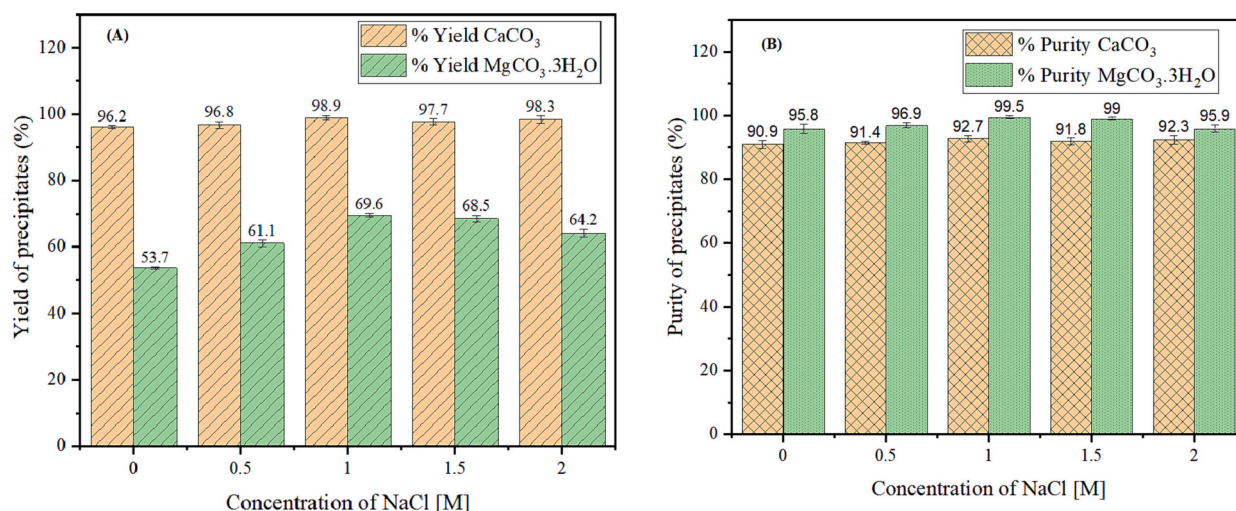


Fig. 1. (A and B): The precipitates yield (%) (A) and purity (%) (B) Against concentration of NaCl in the brine solutions.

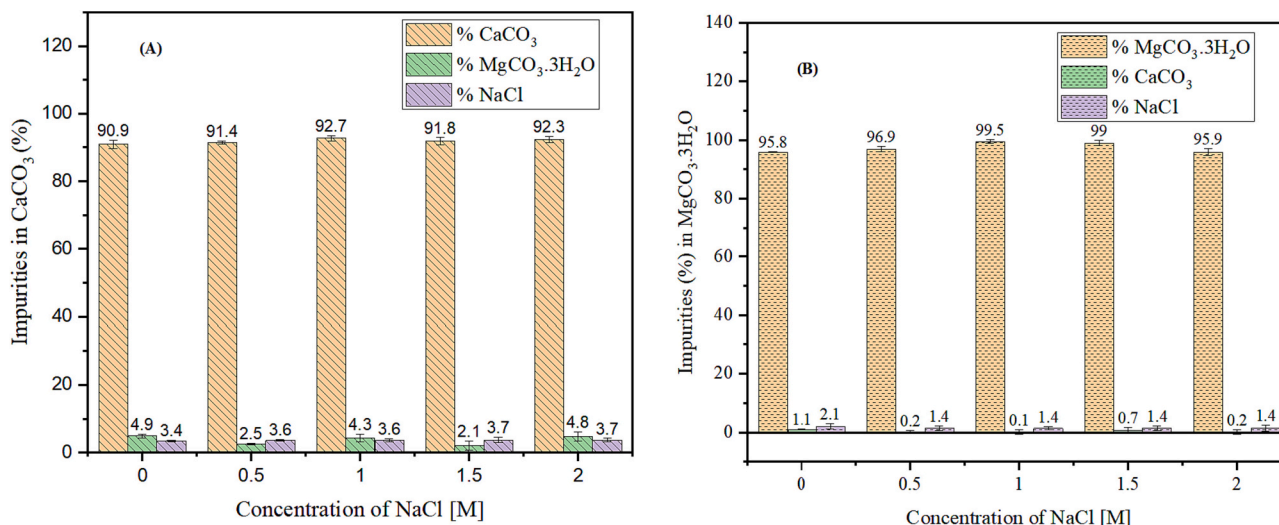


Fig. 2. (A and B): The precipitates impurities (%) in CaCO₃ (A) and MgCO₃·3H₂O (B) against concentration of NaCl in the brine solutions.

2. Material and Methods

2.1. Chemicals used

This study involved the use of NaHCO₃, Na₂CO₃, CaCl₂, MgCl₂·6H₂O, HNO₃, and distilled water and deionized water. All chemicals were used as purchased at analytical grade (≥99% purity) and no further purification treatments were required.

2.2. Experimental design

2.2.1. Preparation of synthetic brine

Table 1 shows the composition of produced water from oilfields. The data were collected from various published reviews and research papers. Based on the level of concentrations in various oilfield-produced water, sodium, calcium, and magnesium are the most ions with high concentrations. Therefore, the design of the experiment under this study aimed to investigate the effects of NaCl on the precipitation of calcium and magnesium carbonates from oilfield-produced water. A total of five synthetic brine solutions were prepared by adding various amounts of (0–2.0 M) NaCl in the mixture of 20,000 Mg/L Ca²⁺ and 10,000 Mg/L Mg²⁺ (Table 2). The control setup was prepared without adding NaCl.

The composition of studied synthetic brine solutions was within the common range of the concentrations of calcium and magnesium ions in oilfield-produced water as reported in different literature (Table 1). Thus, the concentration of calcium ions in the synthetic brine solutions was high compared to that of magnesium ions.

2.2.2. Preparation and optimization of precipitating reagents

To obtain optimum yield and purity of precipitates, it was deemed necessary to perform a preliminary set of experiments to select the proper precipitating reagents [27]. The series of precipitating reagents were prepared from NaHCO₃ and Na₂CO₃ at different concentrations (Table 3). The choice of the reagents comes from the fact that different researchers used the reagents in the precipitation of calcium or magnesium carbonates with promising results [28]. In this study, the precipitating reagents were prepared at different concentrations ranging from 0.5 M to 1.0 M to obtain the optimum reagent concentration. The prepared reagents were tested by sequential precipitating the brine solution to obtain CaCO₃ and MgCO₃·3H₂O at 25 °C and 50 °C. The brine solutions used in preliminary experiments were composed of only 20,000 Mg/L and 10,000 Mg/L Mg²⁺ and Ca²⁺, respectively. Preliminary findings indicated that the concentration of 1.0/0.2 M NaHCO₃/Na₂CO₃ and 1.0 M Na₂CO₃ were optimum to achieve the

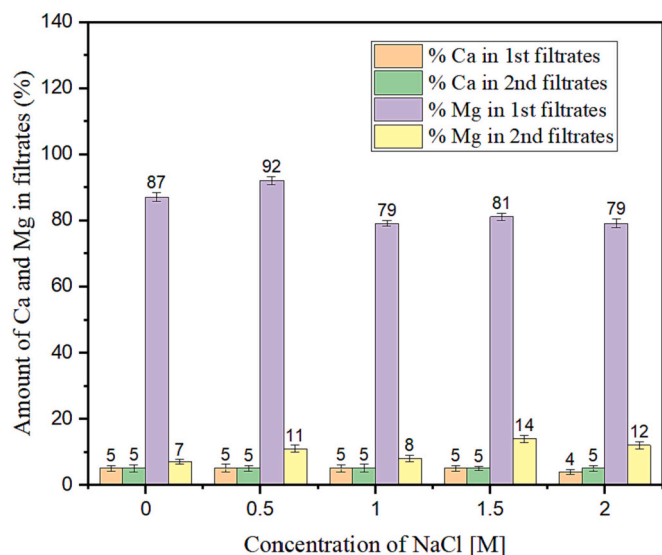


Fig. 3. Amount of Ca^{2+} and Mg^{2+} remained in the first filtrates after removal of CaCO_3 precipitates and in second filtrates after removal of $\text{MgCO}_3 \cdot 3\text{H}_2\text{O}$ precipitates.

highest yield and purity of the precipitates from the brine solutions (Tables 4 and 5). It is suggested that the high pH of the brine solution favors more precipitation of the carbonates [27]. Thus, the observed high yield and purity of precipitates could be associated with high pH levels of 8.93 and 9.72 for 1.0/0.2 M $\text{NaHCO}_3/\text{Na}_2\text{CO}_3$ and 1.0 M Na_2CO_3 , respectively. Additionally, the yield and purity of the precipitates increased at elevated temperatures (50 °C) due to a high reaction rate at the hightemperature. Therefore, the optimized reagent concentrations of 1.0/0.2 M $\text{NaHCO}_3/\text{Na}_2\text{CO}_3$ and 1.0 M Na_2CO_3 from preliminary investigations were used in this study to investigate the precipitation of CaCO_3 and $\text{MgCO}_3 \cdot 3\text{H}_2\text{O}$ at 50 °C, respectively.

2.2.3. Sequential precipitation of carbonates

The precipitation processes were conducted according to Wang et al., 2008 [28] and Zhao et al., 2018 [20] with some modifications. The sequential precipitation experiments were conducted in the simulated temperature environment of an oilfield-produced water at 50 °C using a water bath. This means that oilfield-produced water flows back to the surface from the reservoir in hot conditions [29]. Therefore, the volume of 20 mL of synthetic brine solutions for each experiment was poured into a 250 mL conical flask and heated to 50 °C using a water bath. In the first precipitation step, an equal volume of 20 mL of 1 M $\text{NaHCO}_3/0.2$ M Na_2CO_3 was slowly added to the brine solution using a burette while the brine was continuously stirred at 350 RPM. The pH was recorded initially and at the end of the precipitation process using HANNA pH meter. The pH meter was calibrated using buffer solution at pH of 4.1, 7.0, and 9.2 to ensure correct readings. It was observed the pH of the solutions dropped continuously with the addition of 1 M $\text{NaHCO}_3/0.2$ M Na_2CO_3 up to the end of the precipitation process (Table 6). The decrease in pH as precipitation preceded could be caused by the formation of carbonic acid through the interaction of CO_2 and brine water [27].

The formed precipitates were filtered, washed three times using deionized water to remove the ions, and air-dried at room temperature for 24 h. The second precipitation step was conducted following the same procedures as in the first step. The only difference was the use of filtrates collected from the first step and 1 M Na_2CO_3 . Therefore, the volumes of 20 mL of 1 M Na_2CO_3 were added slowly by using the burette into filtrates (liquids) collected after the first precipitation step. The mixtures were continuously stirred at 350 RPM. Notably, the pH of the solution for each experiment increased with the addition of 1 M Na_2CO_3

in the filtrate during the second precipitation stage.

2.3. Characterization of precipitates and filtrates

2.3.1. MIP AES analysis

The precipitates and filtrates were analyzed with an Agilent Technologies 4100 MIP-AES equipped with an Agilent Technologies 4107 nitrogen generator and a Hydrovane air compressor. Before sample analysis, the standard solutions were prepared as follows. The stock solutions (1000 mg/L) of calcium, magnesium, and sodium were prepared separately by dissolving CaCl_2 , $\text{MgCl}_2 \cdot 6\text{H}_2\text{O}$, and NaCl in distilled water. The multi-element intermediate solution containing 200 mg/L of Ca^{2+} , Mg^{2+} , and Na^+ was prepared by dilution of the stock solutions. The series of seven standard solutions containing 2 mg/L, 10 mg/L, 20 mg/L, 30 mg/L, 40 mg/L, 50 mg/L and 60 mg/L of Ca^{2+} , Mg^{2+} and Na^+ of Ca^{2+} , Mg^{2+} and Na^+ were prepared by further diluting intermediate solution.

Thereafter, the samples of precipitates and filtrates were prepared. The mass of 0.100 g of precipitates was digested using HNO_3 acid and diluted to 100 mL in volumetric flasks. The prepared solutions of precipitates and filtrates were separately filtered by using 0.22 μm micro filter to remove the particulates that could damage the MIP AES plasma torch. The precipitate solutions were further diluted by the factor of 10 and 5 for Ca^{2+} and Mg^{2+} , respectively whereas the filtrate solutions were more concentrated and were diluted by a factor of 500. The precipitates and filtrate were diluted to lower the concentration of ions to the range of the concentrations in standard solutions. Afterward, all prepared samples were analyzed by using MIP-AES. The MIP AES nebulizer pressure was optimized at 120 kPa. The precipitate-based solutions were analyzed at 317.933 nm, 383.933 nm, and 568.820 nm for Ca^{2+} , Mg^{2+} , and Na^+ , respectively. The filtrate samples were analyzed at 616.217 nm, 383.829 nm, and 589.592 nm for Ca^{2+} , Mg^{2+} , and Na^+ , respectively. The lines were selected to avoid interferences from other elements. All samples were analyzed in the triplicate and the results were recorded at average level.

2.3.2. XRD analysis

The samples of dry powder of the precipitates were analyzed using Pan analytical X-ray diffraction (XRD) equipped with a $\text{Cu K}\alpha$ X-ray tube. Each sample was scanned by XRD operating at 45 kV and 40 mA at an angle 2θ ranging from 10° to 60° for 15 min and a scanning rate of 0.021/s. The diffraction pattern of each sample was collected for mineral phase identification. The mineral phases were identified by matching the collected XRD diffraction patterns with the ICDD database (PDF) which was accessed through XRD-X pert high score software.

2.3.3. SEM analysis

The morphology of the synthesized precipitate was analyzed using a JSM-6360LV scanning electron microscope. The finely powdered samples were mounted on 12.5 mm aluminum pin stubs containing adhesive materials. The stubs were inserted in Quorum Q150T ES gold palladium sputter coater instrument for 5 to 7 min to coat the sample with a 10 nm layer of gold and palladium. Afterward, a batch of 10 labeled stubs containing samples was inserted into an SEM sample holder for analysis. All images were scanned at 2 μm and collected for morphological identification.

2.4. Yield and purity determination

The percentage yield and purity of the precipitates were calculated (Eq. 1–3) based on MIP-AES results. The percentage yield of the mineral carbonates was calculated (Eq.1). The actual yield of the precipitates represents the actual weighed mass of obtained dry precipitated from precipitation experiments. The theoretical yield represents the yield obtained from theoretical calculations. The theoretical yields of CaCO_3 and $\text{MgCO}_3 \cdot 3\text{H}_2\text{O}$ were 1.008 g and 1.1353 g, respectively.

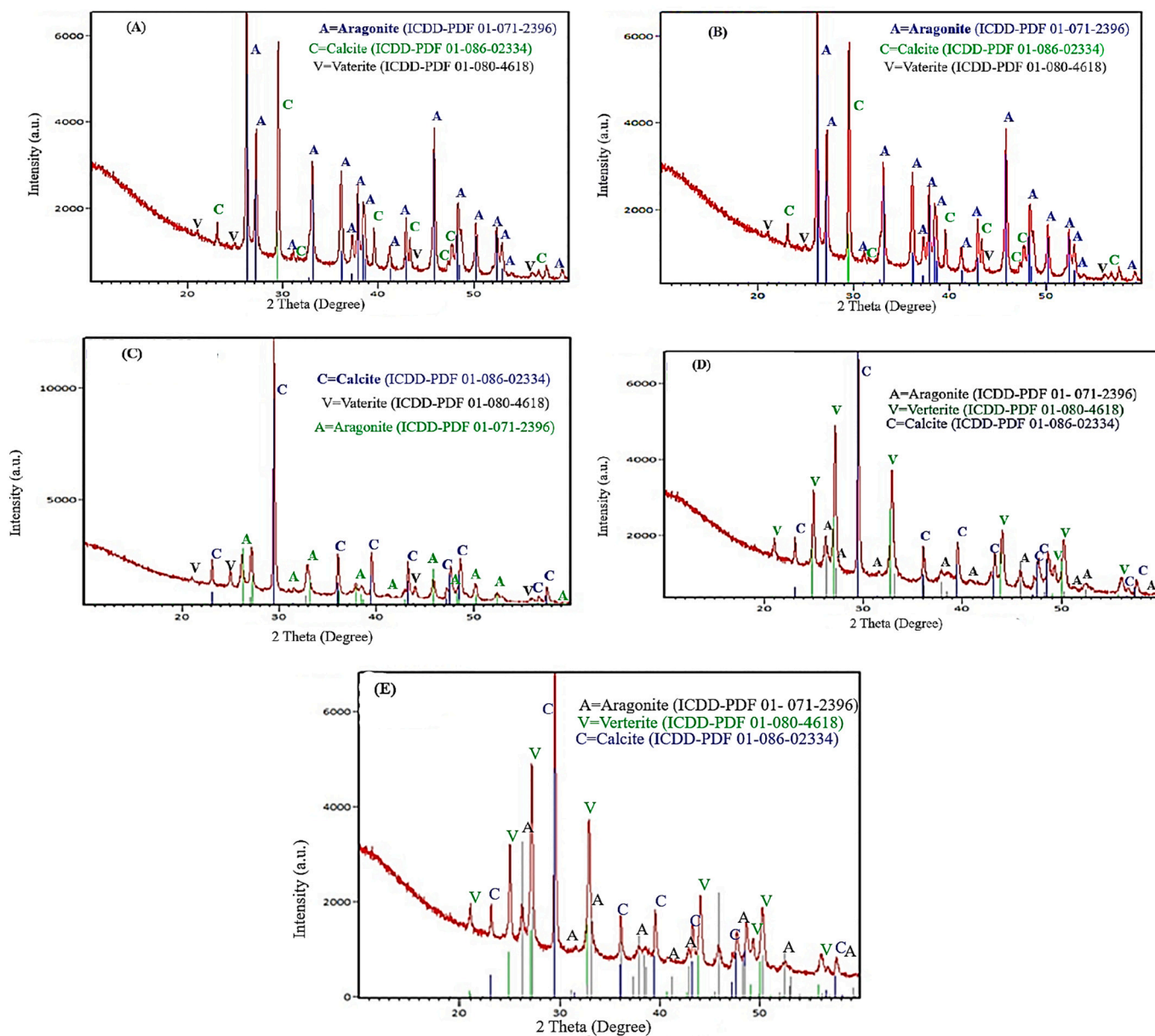


Fig. 4. (A-E): XRD diffraction patterns of CaCO_3 precipitates which were obtained from the brine solutions containing 0.0 M (A), 0.5 M (B), 1.0 M (C), 1.5 (D) and 2.0 M (E) NaCl.

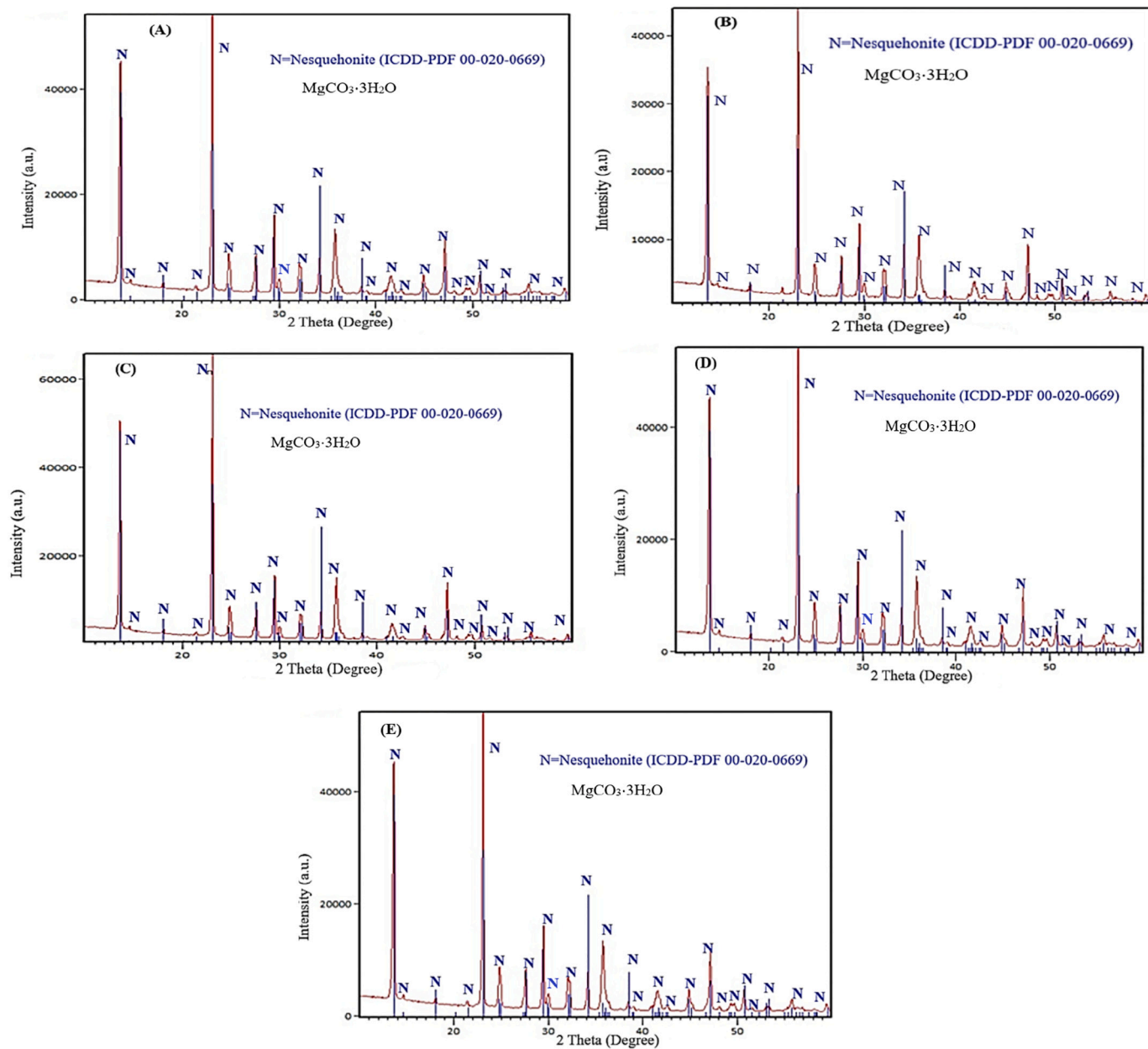


Fig. 5. (A-E): XRD diffraction patterns of $\text{MgCO}_3 \cdot 3\text{H}_2\text{O}$ which were obtained from the brine solutions containing 0.0 M (A), 0.5 M (B), 1.0 M (C), 1.5 (D) and M 2.0 M (E) NaCl.

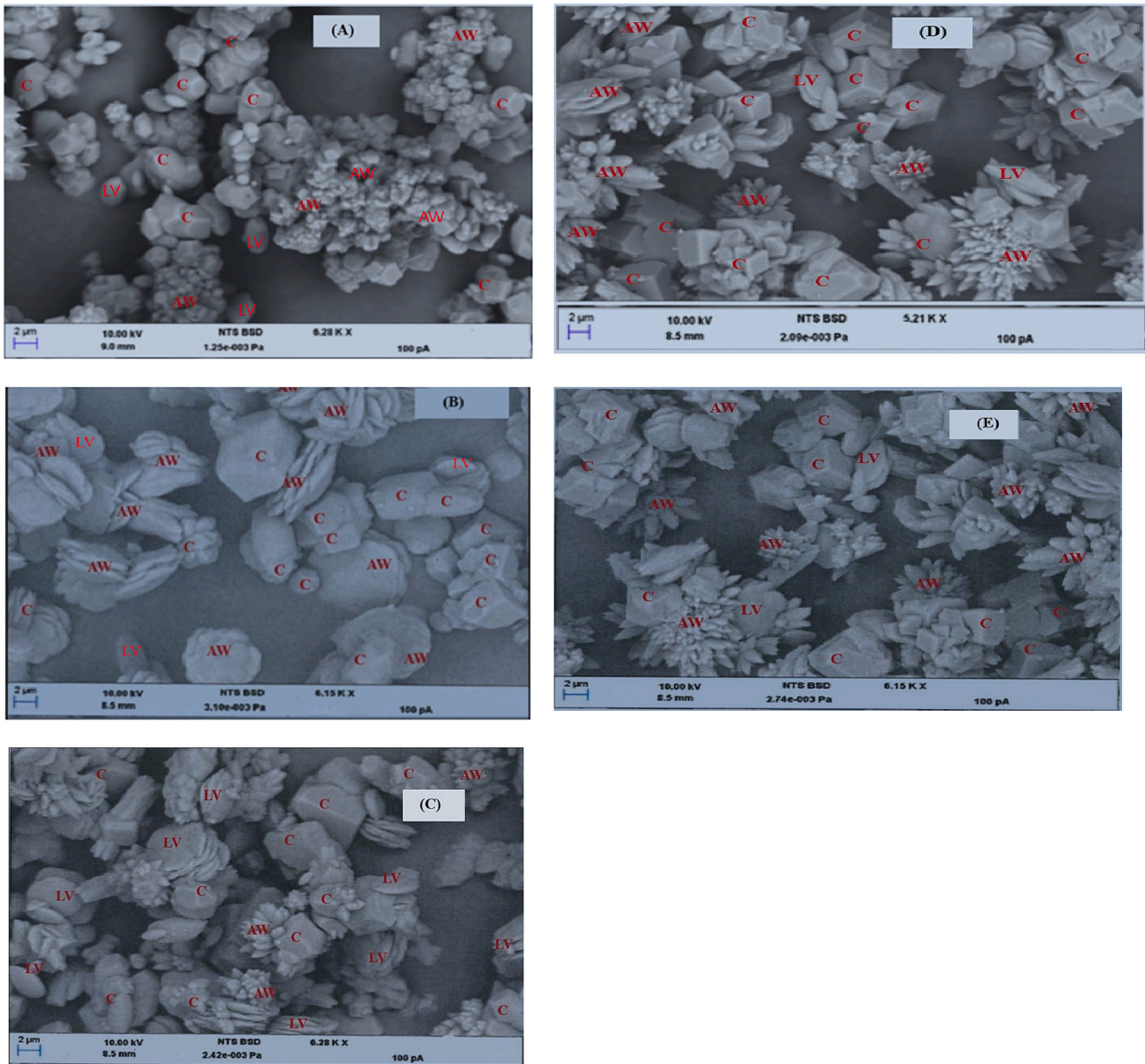


Fig. 6. (A-E): SEM images of CaCO₃ precipitates which were obtained from the brine solutions containing 0.0 M (A), 0.5 M (B), 1.0 M (C), 1.5 (D) and M 2.0 M (E) NaCl.

AW is Aragonite Whiskers
 LV is Lamella Vaterite
 C is Rhombohedral Calcite.

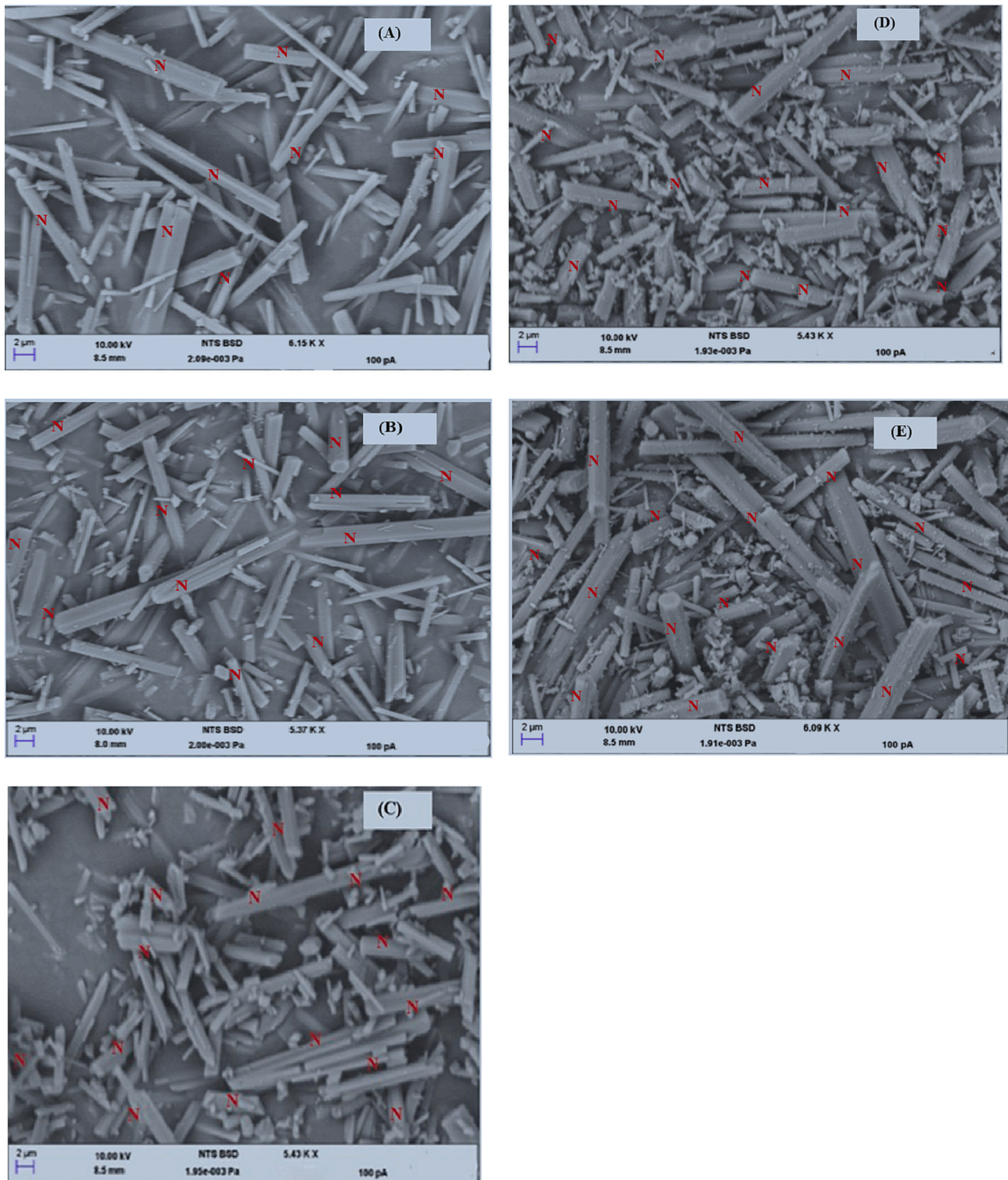


Fig. 7. (A-E): SEM images of $MgCO_3 \cdot 3H_2O$ precipitates which were obtained from the brine solutions containing 0.0 M (A), 0.5 M (B), 1.0 M (C), 1.5 (D) and M 2.0 M (E) NaCl. N is Nesquehonte ($MgCO_3 \cdot 3H_2O$).

Table 7
XRD summary of identified polymorphs of carbonates.

Expt No.	NaCl [M] in the brine solutions	First precipitates (CaCO ₃)	Second precipitates (MgCO ₃ ·3H ₂ O)
1	0.0	Calcite, vaterite, aragonite	Nesquehonite
2	0.5	Calcite, vaterite, aragonite	Nesquehonite
3	1.0	Calcite, vaterite and aragonite	Nesquehonite
4	1.5	Calcite, vaterite and aragonite	Nesquehonite
5	2.0	Calcite, vaterite and aragonite	Nesquehonite

$$\% \text{yield} = \frac{\text{Actual yield}}{\text{Theoretical yield}} \times 100 \quad (1)$$

To quantify the purity of the precipitates, the amount (mg/L) of metal in the solutions was first converted into the mass of metal by multiplying with the volume (L) of the solution. Thus, the mass of pure metal was obtained. Afterward, the mass of the pure metal (Ca or Mg) was converted into the mass targeted pure carbonates (CaCO₃ and MgCO₃·3H₂O) according to eq. 2. The percentage purity of targeted pure carbonates (CaCO₃ and MgCO₃·3H₂O) in the precipitates was calculated according to eq. 3.

$$\text{Mass of pure carbonates} = \frac{\text{Mass of metal (g)}}{\text{Molar mass of metal (g/mol)}} \times \text{Molar mass of carbonate (g/mol)} \quad (2)$$

$$\text{Purity of carbonates (\%)} = \frac{\text{Mass of pure carbonate (g)}}{\text{Mass of dry precipitate obtained from experiments (g)}} \times 100 \quad (3)$$

3. Results and Discussion

3.1. Effects on the yield and purity of carbonates

The results (Fig. 1) indicate the percentage yield and purity of the mineral carbonates obtained from brine solutions by sequential precipitation. The percentage yield of CaCO₃ ranged from 96.2% to 98.9% whereas its purity ranged from 90.9% to 92.7%. The percentage yield of MgCO₃·3H₂O ranged from 53.7% to 64.2% whereas its purity ranged from 95.8% to 99.5%. Furthermore, the yield of CaCO₃ is higher than the yield of MgCO₃·3H₂O. This is due to ions that remained in the filtrates (Fig. 3) after the first precipitation and the removal of CaCO₃ from filtrates. The presence of ions in the filtrates might cause the MgCO₃·3H₂O precipitation inhibition resulting in an observed low percentage yield. The maximum yield and purity were obtained from 1 M NaCl brine solution. That's the maximum yield and purity of CaCO₃ were 98.9% and 92.7%, whereas for MgCO₃·3H₂O were 69.6% and 99.5%, respectively. The result of these findings is similar to the yield of CaCO₃ (>95%) precipitated by mixing 200 mL phosphogypsum, 100 mL NH₃ and CO₂ (flow rate of 0.07 to 0.16) at 20 °C, 45 °C and 80 °C. The reactants concentrations were 2.7 to 4.0 mol/mol NH₃/CaSO₄ and 1.7 to 5.3 mol/mol CO₂/CaSO₄ whereas the pH ranged from 7.2 to 8.0 [17]. On the other side, the observed purity of CaCO₃ was lower compared to 99-% purity of CaCO₃ from the reaction of 400 mL sea water and 100 mL of 10 mmol/L NaCO₃/NaHCO₃ (1.8–8:1) in the temperature ranging

from 30 °C to 70 °C and the pH ranging from 7.9 to 8.9 [30]. The slight difference in purity of CaCO₃ between these findings and others reported in the literature is due to different experimental conditions and reagents which were used. Fig. 2 shows the percentage of impurities that remained in the precipitates. There is no specific trend on the level of impurities in precipitates obtained from 0.0 to 2.0 M NaCl brine solutions. The precipitates of CaCO₃ contained 3.4% to 3.7% NaCl and 2.1% to 4.9% MgCO₃·3H₂O (Fig. 2 A). The precipitates of MgCO₃·3H₂O had a small amount of impurities <2% NaCl and 1% CaCO₃ (Fig. 2 B). Thus, the precipitated MgCO₃·3H₂O was more pure compared to the precipitated CaCO₃.

3.2. Effect on the polymorphs of carbonates

3.2.1. XRD results for CaCO₃ based precipitates

The XRD diffractograms are shown in Fig. 4 A-E. Three polymorphs i. e. vaterite (ICDD-PDF 01-080-4618), calcite (ICDD-PDF 01-086-02334), and aragonite (ICDD-PDF 01-071-2396) were identified by matching the patterns with the library database. The observed diffraction angle 2θ of each identified polymorph is similar to those reported in the literature by Chen and Xiang (2009) [14], Dickinson and McGrath (2001) [16], and Adavi and Dehkordi (2021) [31]. The effect of NaCl on the polymorphs of carbonates is observed. At a low concentration of NaCl (0–0.5 M), the peak intensities of vaterite were lower compared to calcite and aragonite (Fig. 4 A and B). It indicates that vaterite was less favored to precipitate from brine solutions compared to calcite and aragonite. However, as the concentration of NaCl increased from 1 to 2 M, the vaterite peak intensities increased. It indicates that vaterite was more favored formed from the brine solutions as the concentration of NaCl was increased. This observation is in agreement with the earliest

researcher who concluded that vaterite was easily formed from calcium bicarbonate solutions with an increase of NaCl concentration in the solution at elevated temperatures [32]. Additionally, the formation of calcite or vaterite could be influenced by the high pH and Ca²⁺/CO₃²⁻ of the brine solutions. Oral et al., 2018 [33], conducted a study by precipitating CaCO₃ from 4 mL calcium acetate and NaHCO₃ at Ca²⁺/CO₃²⁻ of 5:1, 2:1, 1:2, and 1:3 at pH of 8.0, 10.0, 11.0, 12.0, 13 and temperature of 23 °C in the presence of 20 mL ethylene glycol. They concluded that at high pH and Ca²⁺/CO₃²⁻, vaterite transformed into calcite [33]. Therefore, in comparison to the current study, it can be suggested that vaterite precipitated more in the brine solutions with a slightly low pH of 8.51 to 8.21 caused by an increased concentration of NaCl in the brine solution (Table 6). This is supported by the identified vaterite polymorph in the XRD patterns in Fig. 4 C to D. Nevertheless the findings (Fig. 4 A-E) show that no diffraction peaks correspond to impurities (NaCl and MgCO₃·3H₂O) which could be due to low amounts of impurities (Fig. 2) in the precipitates which could not be detected by XRD.

3.2.2. XRD results for MgCO₃·3H₂O based precipitates

The XRD patterns of magnesium carbonate-based precipitates obtained from filtrate experiments are shown in Figs. 5 (A-E). According to the comparison made between diffractograms and the library database (00–020–0669 ICDD-PDF reference code), results showed that only nesquehonite (MgCO₃·3H₂O) precipitated. Previous findings also reported the formation of similar rod-like nesquehonite at a pH of 9.5 and temperature of 338 K [34]. The presence of various amounts of NaCl in the brine solutions did not change the morphology of nesquehonite. This

result is in agreement with the observed high purity of the precipitates (Fig. 1) and no peak of impurities was identified in the XRD diffractograms. Thus, the precipitate contained a trace amount of impurities (Fig. 2) which could not be detected in XRD analysis. The summary of the carbonate polymorphs identified from XRD diffractograms is indicated in Table 7.

3.3. Effect on the morphology of carbonates

3.3.1. SEM results for CaCO_3 based precipitates

SEM images of analyzed calcium carbonate precipitates are shown in Fig. 6 (A-E). A total of three morphologies of carbonates i.e. lamella vaterite, aragonite whiskers, and rhombohedron calcite were identified [33,35,36]. The image (Fig. 6 A and B) is dominated by rhombohedron calcite and aragonite whiskers. This result is consistent with XRD results showing that the formation of lamella vaterite was less favored in the brine solution containing 0–0.5 M NaCl. At elevated concentrations of 1–2 M NaCl (Fig. 6C-E) lamella vaterite, aragonite whiskers, and rhombohedron calcite were formed which means that an increase in salt concentration in the brine solution facilitated the formation of three morphologies of the precipitates. It is also observed that rhombohedron calcite contains distorted edges and surfaces. This indicates that Mg^{2+} ions in the solution interacted with crystal surfaces during precipitation causing the edges and surface modification [37,38]. Furthermore, the images (Fig. 6C-E) show that aragonite whiskers grow on the surface of calcite. It can be suggested that calcite precipitated first giving the nucleation site for aragonite precipitation.

3.3.2. SEM results for $\text{MgCO}_3 \cdot 3\text{H}_2\text{O}$ based precipitates

Fig. 7(A-E) shows SEM images of magnesium carbonate precipitates. The elongated rod-like structure was observed in the images (Fig. 7 A-E). The formation of a rod-like structure indicates the presence of nesquehonite ($\text{MgCO}_3 \cdot 3\text{H}_2\text{O}$) in the precipitates [11,24,25]. Based on a visual comparison of the SEM images, images (Fig. 7 A-B) show clear, smooth, and elongated crystals than images (Fig. 7 C-E). It shows that the increase in concentration of NaCl (1 M to 2 M) in brine solutions had an influence on the smoothness and length of the crystals but did not change the morphology of $\text{MgCO}_3 \cdot 3\text{H}_2\text{O}$ to other shapes.

4. Conclusion

This study was conducted to investigate the effect of 0–2 M NaCl in brine solution on the sequential precipitation of calcium and magnesium carbonates. The yield of 96.2% to 98.9% CaCO_3 and 53.7% to 69.6% $\text{MgCO}_3 \cdot 3\text{H}_2\text{O}$ with the purity of 90.9% to 92.7% CaCO_3 and 96.0% to 99.5% $\text{MgCO}_3 \cdot 3\text{H}_2\text{O}$ were obtained. The salt concentration of 1 M NaCl in the brine solution offered the maximum yield and purity of 98.9% and 92.7% CaCO_3 and 69.6% and 99.5% $\text{MgCO}_3 \cdot 3\text{H}_2\text{O}$, respectively. Polymorphic and morphological studies revealed that 0–0.5 M NaCl solutions influence more the formation of only two polymorphs of CaCO_3 with various morphologies (aragonite whiskers and rhombohedral calcite). The concentration of 1–2 M NaCl in the brine solutions favors more the formation of three polymorphs of different morphologies (aragonite whiskers, lamella vaterite, and rhombohedral calcite). The variation in NaCl concentration in brine solutions does not affect the polymorph and morphology of magnesium carbonate. Regardless of brine concentration, only elongated rod-like structure nesquehonite ($\text{MgCO}_3 \cdot 3\text{H}_2\text{O}$) was obtained. Furthermore, the increase in salt concentration of the brine solution affects the smoothness and length of the $\text{MgCO}_3 \cdot 3\text{H}_2\text{O}$ crystal.

CRediT authorship contribution statement

Naswibu A. Kasimu: Writing – review & editing, Writing – original draft, Validation, Software, Methodology, Investigation, Funding acquisition, Formal analysis, Data curation, Conceptualization. **Jun Gu:**

Writing – review & editing, Validation, Supervision, Software, Resources, Project administration, Methodology, Investigation, Funding acquisition, Formal analysis, Data curation, Conceptualization.

Declaration of competing interest

The authors declare that they have no known competing financial interests or personal relationships that could have appeared to influence the work reported in this paper.

Data availability

The authors do not have permission to share data.

Acknowledgments

This work was supported by the National Natural Science Foundation of China (grant No. 41972326). Also, thanks are given to Dr. A. Kindness for his support during laboratory analysis.

References

- [1] N. Ahmad, R.E. Baddour, A review of sources, effects, disposal methods, and regulations of brine into marine environments, *Ocean Coast. Manag.* 87 (2014) 1–7, <https://doi.org/10.1016/j.ocecoaman.2013.10.020>.
- [2] S.A. Dastgheib, C. Knutson, Y. Yang, H.H. Salih, Treatment of produced water from an oilfield and selected coal mines in the Illinois Basin, *Int. J. Greenh. Gas Control* 54 (2016) 513–523, <https://doi.org/10.1016/j.ijggc.2016.05.002>.
- [3] S. Jiménez, M.M. Micó, M. Arnaldos, F. Medina, S. Contreras, State of the art of produced water treatment, *Chemosphere* 192 (2018) 186–208, <https://doi.org/10.1016/j.chemosphere.2017.10.139>.
- [4] K.L. Benko, J.E. Drewes, Produced water in the Western United States: geographical distribution, occurrence, and composition, *Environ. Eng. Sci.* 25 (2) (2008) 239–246, <https://doi.org/10.1089/ees.2007.0026>.
- [5] J. Neff, K. Lee, E.M. DeBlois, *Produced Water: Overview of Composition, Fates, and Effects*, Springer, New York, 2011, https://doi.org/10.1007/978-1-4614-0046-2_1.
- [6] T. Chen, Influence of Mg^{2+} on CaCO_3 formation—bulk precipitation and surface deposition, *Chem. Eng. Sci.* 61, no. Elsevier (2006) 5318–5327, <https://doi.org/10.1016/j.ces.2006.04.007>.
- [7] O. Abessi, *Brine Disposal and Management-Planning, Design, and Implementation, Sustainable, Desalination Handbook*, Butterworth-Heinemann, 2018, <https://doi.org/10.1016/B978-0-12-809240-8.00007-1>.
- [8] J. V. Del Bene, G. Jirka, and J. Largier, “Ocean brine disposal,” *Desalination*, vol. 97, no. 1–3, pp. 365–372, Aug. 1994, doi:[https://doi.org/10.1016/0011-9164\(94\)00100-6](https://doi.org/10.1016/0011-9164(94)00100-6).
- [9] M. Ahmed, A. Arakelb, D. Hoey, M.R. Thumarukudyd, M.F.A. Goosen, M. Haddabi, A. Belushi, Feasibility of salt production from inland RO desalination plant reject brine: a case study, *Desalination* 158 (1–3) (2003) 109–117, [https://doi.org/10.1016/S0011-9164\(03\)00441-7](https://doi.org/10.1016/S0011-9164(03)00441-7).
- [10] British calcium carbonate federation B.C.C.F. BCCF UK, <https://calcium-carbonate.org.uk/calcium-carbonate/calcium-uses/>, 2019.
- [11] F.P. Glasser, G. Jauffret, J. Morrison, J.-L. Galvez-Martos, N. Patterson, M.S.-E. Imbabi, Sequestering CO₂ by mineralization into useful nesquehonite-based products, *Front. Energy Res.* 4 (February) (2016) 1–7, <https://doi.org/10.3389/fenrg.2016.00003>.
- [12] M. Hánchez, V. Prigiobbe, R. Baciocchi, M. Mazzotti, Precipitation in the mg-carbonate system-effects of temperature and CO₂ pressure, *Chem. Eng. Sci.* 63 (4) (2008) 1012–1028, <https://doi.org/10.1016/j.ces.2007.09.052>.
- [13] W. Cheng, Z. Li, G.P. Demopoulos, Effects of temperature on the preparation of magnesium carbonate hydrates by reaction of MgCl_2 with Na_2CO_3 , *Chin. J. Chem. Eng.* 17 (4) (2009) 661–666, [https://doi.org/10.1016/S1004-9541\(08\)60260-8](https://doi.org/10.1016/S1004-9541(08)60260-8).
- [14] J. Chen, L. Xiang, Controllable synthesis of calcium carbonate polymorphs at different temperatures, *Powder Technol.* 189 (1) (2009) 64–69, <https://doi.org/10.1016/j.powtec.2008.06.004>.
- [15] C.A. Weiss, R. Moser, M. Chandler, P. Malone, Influence of temperature on calcium carbonate polymorph formed from ammonium carbonate and calcium acetate, *J. Nanotechnol. Smart Mater.* 1 (2014) 1–6, <https://doi.org/10.17303/JNSM.2014.105>.
- [16] S.R. Dickinson, K.M. McGrath, Quantitative determination of binary and tertiary calcium carbonate mixtures using powder X-ray diffraction, *Analyst* 126 (7) (2001) 1118–1121, <https://doi.org/10.1039/b103004n>.
- [17] H. Mattila, R. Zevenhoven, Mineral carbonation of phosphogypsum waste for production of useful carbonate and sulfate salts 3 (November) (2015) 1–8, <https://doi.org/10.3389/fenrg.2015.00048>.
- [18] G. Costa, S. Teir, Performance of separation processes for precipitated calcium carbonate produced with an innovative method from steelmaking slag and carbon dioxide, *Front. Energy Res.* 4 (February) (2016), <https://doi.org/10.3389/fenrg.2016.00006>.

- [19] J. Jeon, M. Kim, CO₂ storage and CaCO₃ production using seawater and an alkali industrial, *Chem. Eng. J.* 378 (May) (2019) 122180, <https://doi.org/10.1016/j.cej.2019.122180>.
- [20] Y. Zhao, M. Wu, X. Guo, Y. Zhang, Z. Ji, J. Wang, J. Liu, J. Liu, Z. Wang, Q. Chi, J. Yuan, Thorough conversion of CO₂ through two-step accelerated mineral carbonation in the MgCl₂-CaCl₂-H₂O system, *Sep. Purif. Technol.* 210 (2019) 343–354, <https://doi.org/10.1016/j.seppur.2018.08.011>.
- [21] J. Pichtel, Oil and gas production wastewater: soil contamination and pollution prevention, *Appl. Environ. Soil Sci.* 2016 (2016), <https://doi.org/10.1155/2016/2707989>.
- [22] A. Rahman, S. Agrawal, T. Nawaz, S. Pan, T. Selvaratnam, A review of algae-based produced water treatment for biomass and biofuel production, *Water (Switzerland)* 12 (9) (2020) 1–27, <https://doi.org/10.3390/W12092351>.
- [23] Y. Liu, H. Lu, Y. Li, H. Xu, Z. Pan, P. Dai, H. Wang, Q. Yang, A review of treatment technologies for produced water in offshore oil and gas fields, *Sci. Total Environ.* 775 (2021) 145485, <https://doi.org/10.1016/j.scitotenv.2021.145485>.
- [24] J.A. Veil, Produced Water Management Options and Technologies, in: K. Lee, J. Neff (Eds.), *Produced Water*, Springer, New York, NY, 2011, https://doi.org/10.1007/978-1-4614-0046-2_29.
- [25] S. Al-Kindi, S. Al-Bahry, Y. Al-Wahaibi, U. Taura, S. Joshi, Partially hydrolyzed polyacrylamide: enhanced oil recovery applications, oil-field produced water pollution, and possible solutions, *Environ. Monit. Assess.* 194 (12) (2022), <https://doi.org/10.1007/s10661-022-10569-9>.
- [26] S. Jiménez, M.M. Micó, M. Arnaldos, F. Medina, S. Contreras, State of the art of produced water treatment, *Chemosphere* 192 (2018) 186–208, <https://doi.org/10.1016/j.chemosphere.2017.10.139>.
- [27] G.M. Ayoub, R.M. Zayyat, M. Al-Hindi, Precipitation softening: a pretreatment process for seawater desalination, *Environ. Sci. Pollut. Res.* 21 (4) (2014) 2876–2887, <https://doi.org/10.1007/s11356-013-2237-1>.
- [28] Y. Wang, Z. Li, G.P. Demopoulos, Controlled precipitation of nesquehonite (MgCO₃·3H₂O) by the reaction of MgCl₂ with (NH₄)₂CO₃, *J. Cryst. Growth* 310 (6) (2008) 1220–1227, <https://doi.org/10.1016/j.jcrysgro.2008.01.002>.
- [29] I. Abdallah, Cost effective treatment of produced water using co-produced energy sources, *Proc. - SPE Annu. Tech. Conf. Exhib.* 7 (2014) 5612–5620, <https://doi.org/10.2118/173475-stu>.
- [30] H. Jin Sun, X. Guo, S. Wang, J. Bi, Z. Ji, Y. Zhao, Precipitation and in-situ surface modification of calcium carbonate in synthetic seawater: polymorph control, crystallization kinetics, and hydrophobic vaterite preparation, *J. Environ. Chem. Eng.* 11 (3) (2023) 110019, <https://doi.org/10.1016/j.jece.2023.110019>.
- [31] K. Adavi and A. Molaei Dehkordi, “Synthesis and polymorph controlling of calcite and aragonite calcium carbonate nanoparticles in a confined impinging-jets reactor,” *Chem. Eng. Process. - Process Intensif.*, vol. 159, no. September 2020, p. 108239, 2021, doi:<https://doi.org/10.1016/j.cep.2020.108239>.
- [32] Y. Kitano, A study of the polymorphic formation of calcium carbonate in thermal springs with an emphasis on the effect of temperature, *Bull. Chem. Soc. Jpn.* 35 (12) (1962) 1980–1985, <https://doi.org/10.1246/bcsj.35.1980>.
- [33] Ç.M. Oral, B. Ercan, Influence of pH on morphology, size and polymorph of room temperature synthesized calcium carbonate particles, *Powder Technol.* 339 (2018) 781–788, <https://doi.org/10.1016/j.powtec.2018.08.066>.
- [34] Z. Zhang, Y. Zheng, Y. Ni, Z. Liu, J. Chen, X. Liang, Temperature- and pH-Dependent Morphology and FT-IR Analysis of Magnesium Carbonate Hydrates, *J. Phys. Chem. B* 110 (26) (2006) 12969–12973, <https://doi.org/10.1021/jp061261j>.
- [35] M. Altiner, M. Yildirim, Production and characterization of synthetic aragonite prepared from dolomite by eco-friendly leaching-carbonation process, *Adv. Powder Technol.* 28 (2) (2017) 553–564, <https://doi.org/10.1016/j.apt.2016.10.024>.
- [36] P.D. Natsi, S.G. Rokidi, P.G. Koutsoukos, Precipitation of calcium carbonate (CaCO₃) in water-monoethylene glycol solutions, *Ind. Eng. Chem. Res.* 58 (12) (2019) 4732–4743, <https://doi.org/10.1021/acs.iecr.8b04180>.
- [37] J.M. Astilleros, L. Fernández-díaz, A. Putnis, The role of magnesium in the growth of calcite: an AFM study, *Chem. Geol.* 271 (1–2) (2010) 52–58, <https://doi.org/10.1016/j.chemgeo.2009.12.011>.
- [38] Y. Zhang, R.A. Dawe, Influence of Mg²⁺ on the kinetics of calcite precipitation and calcite crystal morphology, *Chem. Geol.* 163 (1–4) (2000) 129–138, [https://doi.org/10.1016/S0009-2541\(99\)00097-2](https://doi.org/10.1016/S0009-2541(99)00097-2).